IEICE TRANS. COMMUN., VOL.E103–B, NO.1 JANUARY 2020

PAPER

Proposal of Instantaneous Power-Line Frequency Synchronized Superimposed Chart for Communications Quality Evaluation of broadband PLC System

Kenji KITA[†a)], ***Member***, **Hiroshi GOTOH**[††], ***Student Member***, **Hiroyasu ISHIKAWA**[†††], ***Senior Member***, ***and*** **Hideyuki SHINONAGA**[†,††], ***Fellow***

SUMMARY Power line communications (PLC) is a communication technology that uses a power-line as a transmission medium. Previous studies have shown that connecting an AC adapter such as a mobile phone charger to the power-line affects signal quality. Therefore, in this paper, the authors analyze the influence of chargers on inter-computer communications using packet capture to evaluate communications quality. The analysis results indicate the occurrence of a short duration in which packets are not detected once in a half period of the power-line supply: named communication forbidden time. For visualizing the communication forbidden time and for evaluating the communications quality of the inter-computer communications using PLC, the authors propose an instantaneous power-line frequency synchronized superimposed chart and its plotting algorithm. Further, in order to analyze accurately, the position of the communication forbidden time can be changed by altering the initial burst signal plotting position. The difference in the chart, which occurs when the plotting start position changes, is also discussed. We show analysis examples using the chart for a test bed data assumed an ideal environment, and show the effectiveness of the chart for analyzing PLC inter-computer communications.

key words: *PLC, packet capture analysis, visualization, communication quality evaluation*

1. Introduction

The popularity of Internet services in recent years has made it common to build a local area network (LAN) environment in the home. Wireless LANs are most used, but because of the distance from an access point and the influence of radio wave shielding objects, radio wave blocking may degrade communicate quality. Another approach is to install a wired LAN, but many people feel resistance to extending LAN cables throughout homes. In such a case, power line communications (PLC) is one way to construct a LAN environment in homes. PLC uses the power-lines already laid in the house to realize communication links. Therefore, it is possible to set easily a LAN environment by inserting the PLC adapter into the power outlet, and PLC is expected as a construction method of a network environment in homes as well as wireless LAN and wired LAN. The concept of PLC was already known in 1950 [1], but a high-speed transmission using a high-speed PLC in frequency bands of several MHz to several tens MHz have become possible only recently. In Japan, high-speed PLC was restricted to indoor use in 2006 by limited the frequency bands to 2 to 30 MHz and considering the influence on the amateur radio due to leaky radio waves from the power-line. Most high-speed PLC systems used in Japan comply with one of three standards, High Definition Power Line Communication (HD-PLC) by HD-PLC Alliance [2], HomePlug AV by HomePlug Alliance [3] and UPA by Universal Powerline Association [4]. Although these PLC standards are poorly compatible, plans to enable communication regardless of PLC standards and vendors are in progress [5]. In recent years, with the improvement of PLC, it became possible to transmit digital high-vision videos, so it is expected to be applied to home networks mainly for home Audio-Visual services [6]. However, as a matter of PLC, it has been showed that when a load, especially an alternating current (AC) adapter such as a mobile phone charger, is connected to the power-line, PLC is affected and the throughput decreases [7]. In addition, Corripio et al. have measured the influence of home electronics including chargers on PLC using multi-tone, and showed that two types of transfer function appear in a half period of the power-line period [8]. Furthermore, Umehara et al. have showed that a charger generates two kinds of transfer function in a half period of the power-line period by using the pulse signal [9]. However, these are the influences that a charger gives in the power-line, and it is not clear how a charger affects actual computer communications. Therefore, the authors analyze the influence of a charger on inter-computer communications by packet capture. From the analysis, we clarify a section where packets are not detected once in a half period of the power-line period: named communication forbidden time. In order to visualize the influence of a charger on inter-computer communications such a communication forbidden time, we propose an instantaneous power-line frequency synchronized superimposed chart in this paper, and it is possible to visualize the characteristics of the inter-computer communication typified by a communication forbidden time when the charger is connected, and also the difference between the communication statuses when the charger is connected or not. As a structure of this paper, we explain a commu-

Manuscript received February 20, 2019.
Manuscript revised June 11, 2019.
Manuscript publicized July 18, 2019.

[†]The authors are with Faculty of Science and Engineering, Toyo University, Kawagoe-shi, 350-8585 Japan.
[††]The authors are with Graduate School of Science and Engineering, Toyo University, Kawagoe-shi, 350-8585 Japan.
[†††]The author is with College of Engineering, Nihon University, Koriyama-shi, 963-8642 Japan.
a) E-mail: kita@toyo.jp

DOI: 10.1587/transcom.2019EBP3049

nication forbidden time clarified by the analysis in Sect. 2. Next, the instantaneous power-line frequency synchronized superimposed chart and its plotting algorithm are described in detail in Sect. 3. Further, the chart can be plotted by changing the initial burst signal plotting position in order to analyze accurately, and we discuss the influence on the chart caused by the initial burst signal plotting position in Sect. 4. Finally in Sect. 5, an example of analysis using the instantaneous power-line frequency synchronized superimposed chart is shown, and the effectiveness of the proposed chart is shown.

2. Inter-Computer Communications Analysis by Packet Capture

A method to analyze the influence of a charger to inter-computer communications by packet capture is shown. A communication forbidden time not detecting packets is indicated using packet capture analysis.

2.1 Experiment System and Method

Figure 1 shows an ideal test bed experiment system using a 100 m VVF (Vinyl insulated Vinyl sheathed Flat-type) cable. The commercial power-line frequency is 50 Hz, that is, one period is about 20 msec and a half period is about 10 msec. In this system, a noise-cut transformer is used so that the influence of frequency measurement equipment for measuring the power-line frequency does not affect. The digital multimeter outputs the power-line frequency measured for 100 msec at intervals of 220 msec [10]. However, in fact it was randomly outputting at 218 msec or 219 msec intervals. An AC adapter, feature phone charger, is connected to the outlet to which the Receiving PLC device is connected. The influence of the AC adapter to inter-computer communications is examined by packet capture analysis. This experiment used User Datagram Protocol (UDP) to communicate. Packets were generated by packet generation software iperf [11] and transmitted from the transmitting PC (TxPC) at the preset UDP transmission speed of 30 Mbit/s. PLC devices were used HD-PLC and the packets were captured by the receiving PC (RxPC) via the VVF cable. Wireshark [12] was used as the capture software, also used to measure packet reception times. The main specifications of each device are shown in the Table 1.

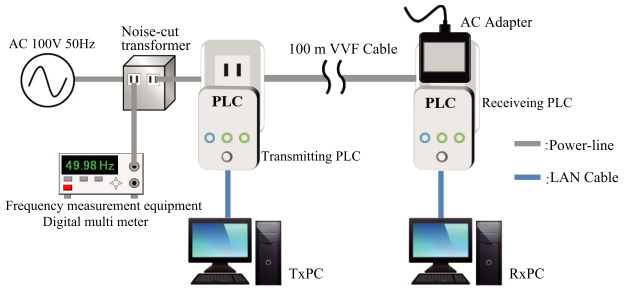

Fig. 1 Experiment system.

2.2 Communication Forbidden Time

Figure 2 shows that the relationship between the packet identity number (Packet ID) and transmitted and received time. In each case, the horizontal axis is the packet capture time, and the vertical axis is the Packet ID attached by Wireshrak of the TxPC or RxPC. Figures 2(a) and (b) respectively show the packet transmission time captured by the TxPC and the packet reception time captured by the RxPC when the charger is disconnected. According to the specifications

Table 1 Main specifications.

PLC device	HD-PLC Panasonic BL-PA310 [13]
OS of TxPC	Ubuntu ver. 13.10 [14]
OS of RxPC	Ubuntu ver. 14.04LTS [14]
Packet transmission software	iperf ver. 2.0.5 [11]
Packet size	1512 bytes
TxPC packet capture software	Wireshark ver. 1.10.2 [12]
RxPC packet capture software	Wireshark ver. 1.10.6 [12]
Category of LAN Cable	6A
Wired LAN connection speed	100Base-TX
Digital multi meter	ADCMT 7352E [10]
Noise-cut trans.	UNION MNR-D-9-1010 [15]
AC adapter	feature phone charger

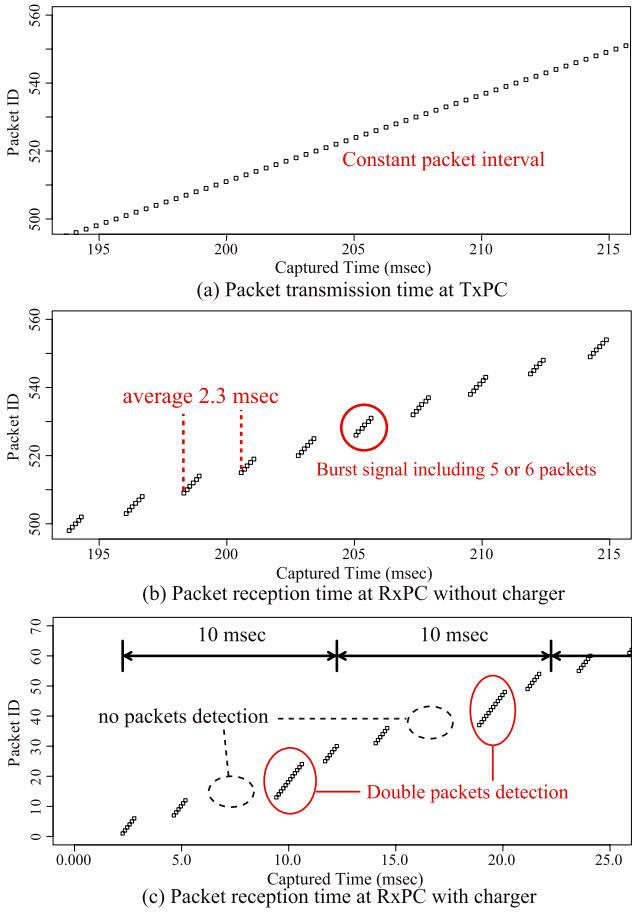

(a) Packet transmission time at TxPC
(b) Packet reception time at RxPC without charger
(c) Packet reception time at RxPC with charger

Fig. 2 Relationship between Packet ID and transmitted and received time.

of the medium access control (MAC) layer of inter-HD-PLC communications within a power-line [16], packets transmitted from TxPC are aggregated as a maximum of 31 subframes in a single data frame at the Transmitting PLC and are transmitted in the power-line. Since C-Mark, which is the 16-byte code to distinguish subframes placed between segment blocks, is inserted between subframes at the Transmitting PLC, the Receiving PLC can separate the subframes according to C-Mark and transmit them as a single packet on the LAN cable. Therefore, as shown in Fig. 2(a) and (b), although the packet interval at TxPC is constant, the RxPC captures several packets as a burst signal. The previous study have shown that the burst signal inclusion packets at the preset UDP transmission speed of 30 Mbit/s is on average 5 or 6, and the average of the burst signal head packet interval is 2.3 msec [17]. That is, it is estimated that the Transmitting PLC aggregates 5 or 6 packets and transmits them as a single signal in the power-line in an interval of 2.3 msec. Figure 2(c) shows the packet reception time at the RxPC when the charger is connected. Comparing Fig. 2(b) with(c), burst signals are not detected at the RxPC in the duration indicated by the broken circle. We clarified that burst signals are not detected in such duration in inter-computer communications using PLC when the charger is connected: named *communication forbidden time*. Communication forbidden time has occurred once at about 10 msec, which is a half period of the power-line period. In the previous study, Umehara et al. have suggested that the transfer function of the power-line changes once a half period of the power-line period when the charger is connected [9], and we suppose that the communication forbidden time is also related to a half period of the power-line period and the change of the transfer function. Furthermore, the number of packets in the burst signal immediately after the communication forbidden time is about 10 to 12, which is about double for 5 and 6 in the normal. According to the specifications of MAC layer of inter-HD-PLC communications [16], the Receiving PLC sends to the Transmitting PLC the Acknowledgment including the "Result Map field" indicating whether the subframe in the data frame has been correctly received. Since the Result Map field corresponds to each subframe, the Transmitting PLC can recognize subframes that could not be normally received. Thereafter, the Transmitting PLC aggregates subframes which could not be normally received in addition to subframes scheduled to be transmitted in the next data frame. In addition, although the PLC adapter has a function to execute channel estimation when degradation of the power-line channel characteristics is detected [16], it does not have a function to detect changes in the power-line channel characteristics in advance and to suspend transmission. Considering all of these things, the Transmitting PLC transmit packets even during the communication forbidden time but can not be received normally by the Receiving PLC, and since the Transmitting PLC has re-transmitted, the number of packets captured immediately after the communication forbidden time increases. Although not observed directly in the power-line, it can be estimated from packet capture analysis of inter-computer communications. In this way, the communication forbidden time occurring when the charger is connected has some influence on the communication quality of inter-computer communications using PLC. Therefore, focusing on the communication forbidden time that occurs once in a half period of the power-line period, we propose an instantaneous power-line frequency synchronized superimposed chart as a method to visualize the communication forbidden time and to analyze the influence on PLC.

3. Plotting Algorithm of Instantaneous Power-Line Frequency Synchronized Superimposed Chart

A plotting algorithm of the instantaneous power-line frequency synchronized superimposed chart and its validity by a plotting simulation are described in detail.

3.1 Instantaneous Power-Line Frequency Synchronized Superimposed Chart

The instantaneous power-line frequency synchronized superimposed chart (referred to as *Proposed Chart*) is two-dimensional chart with the horizontal axis as a half period of the power-line period and the vertical axis as the capture time, briefly. Focusing on that the burst signal is received in the RxPC as shown in Fig. 2(b) and (c), the reception time of the burst signal head packet is plotted as a representative on the Proposed Chart. As a method of distinguishing the burst signal, as shown in Fig. 2(b) and (c), one burst signal is defined as a packet in which a narrow interval between packets is consecutive from a packet after a large inter-packet interval, and as a next burst signal when the interval between packets becomes large. At this time, the number of the burst signal inclusion packets and packet intervals are also held as data in association with each burst signal. By reflecting these data in the Proposed Chart as necessary, more detailed analysis becomes possible.

3.2 Plotting Algorithm

A plotting algorithm of the Proposed Chart is 6 Steps.

Step 1 Determination of initial burst signal plotting position: The horizontal axis represents a half period of the power-line period calculated from the instantaneous power-line frequency, which is referred to as *Superimposed Period*. Superimposed Period SP_1 of the initial burst signal is calculated from the instantaneous power-line frequency F_1 at the reception time of the initial burst signal. Initial burst signal plotting position $IniP$ is arbitrarily determined within the following range, and this is set as the plotting point on the horizontal axis, which is referred to *Superimposed Time* ST_1.

$$SP_1 = \frac{1}{2F_1}. \tag{1}$$

$$ST_1 = IniP \qquad (0 \leqq IniP < SP_1). \tag{2}$$

The initial burst signal ID_1 reflecting $IniP$ on the Proposed Chart is plotted.

Step 2 Set burst signal ID initial value:
The initial value of the burst signal ID n is set to 2.
Step 3 Calculation of Superimposed Time:
Burst signal reception time interval $Int_{Burst\ n}$ is calculated from n-th burst signal reception time $T_{Burst\ n}$ and $(n-1)$-th $T_{Burst\ n-1}$. Further, n-th burst signal Superimposed Time ST_n is obtained by adding burst signal reception time interval $Int_{Burst\ n}$ to $(n-1)$-th burst signal Superimposed Time ST_{n-1}.

$$Int_{Burst\ n} = (T_{Burst\ n} - T_{Burst\ n-1}). \tag{3}$$

$$ST_n = ST_{n-1} + Int_{Burst\ n}. \tag{4}$$

Step 4 Calculation of Superimposed Period:
SP_n is calculated from F_n at the reception time of the n-th burst signal.

$$SP_n = \frac{1}{2F_n}. \tag{5}$$

Step 5 Judgment of Superimposed Time repetition:
When ST_n is equal to or longer than SP_n, ST_n is corrected as follows:

$$\text{while } ST_n \geqq SP_n,\ \ ST_n = ST_n - SP_n. \tag{6}$$

If the burst signal reception time interval becomes larger due to the influence of the communications forbidden time and ST_n exceeds twice SP_n, Eq. (6) is repeated until ST_n becomes less than SP_n.
Step 6 Judgment of algorithmic termination:
If burst signal ID n is equal to the total number of burst signals n_{max}, this algorithm is ended normally. If n is less than n_{max}, n is added to 1 and the algorithm returns to **Step 3**.

$$\text{if } n{=}\ n_{max} \text{ then END else } n{=}n{+}1, \text{ return to } \textbf{Step 3}. \tag{7}$$

In the above, the Proposed Chart is plotted. The flowchart of the plotting algorithm is shown in the Fig. 3. This algorithm will be described in detail with reference to Fig. 4. The green circle on the left side is sequentially arranged according to the reception time of the burst signals. The numbers inside the circles indicate the burst signal ID. The lower yellow circles indicate the Superimposed Time. The red circle in the Proposed Chart is the point to be plotted. The blue line on the right shows the fluctuation of the instantaneous power-line frequency acquired by the digital multimeter. First, in order to determine the initial burst signal plotting position in **Step 1**, the instantaneous frequency at the reception time of the first burst signal is acquired from blue line, and Superimposed Period SP_1 is calculated. The Superimposed Period is one-half of the inverse of the power-line frequency. Initial burst signal plotting position $IniP$, so that means Superimposed Time ST_1, is determined within the range of SP_1 and plotted on the Propose Chart. The point is the red circle ID_1. Next, n is set to 2 in **Step 2**, and the plotting position determination of the burst signal ID_2 is started. In **Step 3**, burst signal reception time interval $Int_{Burst\ 2}$ is calculated from burst signal reception time $T_{Burst\ 2}$ of the burst signal

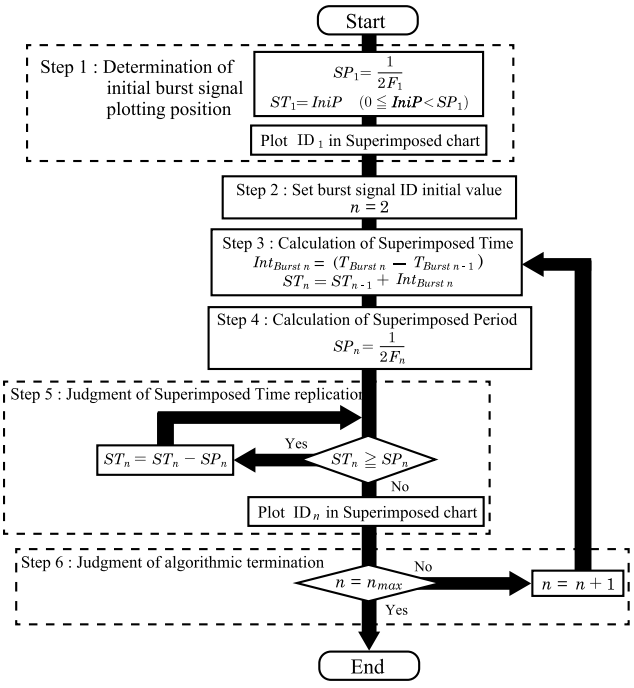

Fig. 3 Flowchart of plotting algorithm.

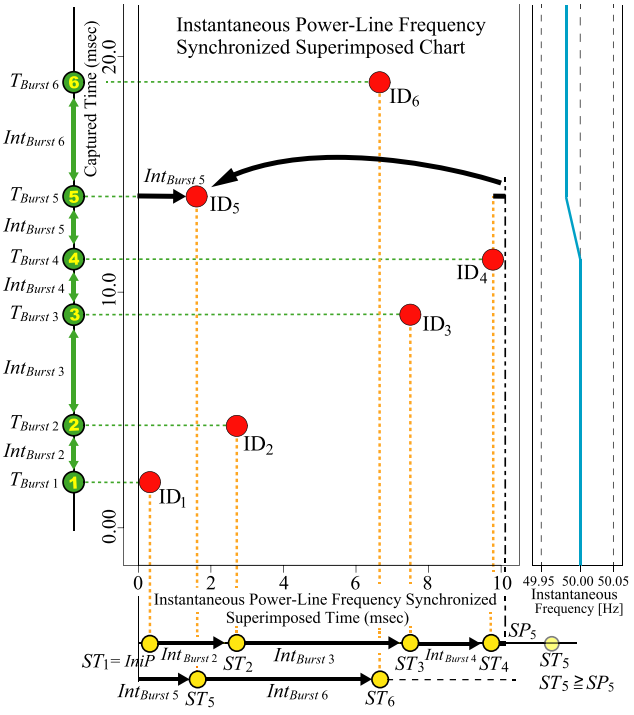

Fig. 4 Plotting procedure.

ID_2 (green circle No. 2) and $T_{Burst\ 1}$ of the burst signal ID_1 (green circle No. 1). $Int_{Burst\ 2}$ and ST_1 are added in the direction of the horizontal axis and set as ST_2, this is the yellow circle. In **Step 4**, from the instantaneous power-line frequency on the right side, the frequency when the burst signal ID_2 was received is acquired and SP_2 is calculated. In

Step 5, ST_2 and SP_2 are compared. In this case, since SP_2 is larger, the red circle ID_2 is plotted at the intersection point of ST_2 and $T_{Burst\ 2}$. ST_n may exceed SP_n, as in ST_5 and SP_5 in Fig. 4. In this case, as in the yellow circle ST_5, The value obtained by subtracting SP_5 from ST_5 is redefined as ST_5 and plotted on the Proposed Chart. It is determined in **Step 6** whether all the burst signals are plotted, and **Step 3** to **Step 6** are repeated until those are plotted. In this way, the Proposed Chart is completed.

3.3 Plot Simulation

A plot simulation using the instantaneous power-line frequency generated by a computer in order to confirm the validity of the proposed algorithm is shown. Table 2 shows the simulation condition. The burst signal interval was 2.3 msec which is the average interval value of the HD-PLC system at preset UDP transmission speed of 30 Mbit/s. The number of burst signals is 80,000, which corresponds to 184 seconds when transmitting at 2.3 msec intervals. The power-line frequency was set to be an average 50 Hz and a standard deviation ±0.02 Hz. This standard deviation ±0.02 Hz was reference to the annual standard deviation target value of the average value per minute in the United States and the stay ratio in Europe [18]. The digital multimeter used to acquire the instantaneous power-line frequency outputs data once in 218 msec or 219 msec. Therefore, it is changed in the simulation as well as the experiment. For simplification of simulation, it is assumed that the communication forbidden time occurs between an AC power supply phase angle of 60 degrees at which the AC charger starts charging and 90 degrees at which charging ends, and these phase angles are roughly estimated using the reference [19]. This is because when the charger starts or ends charging, the transfer function in the power-line abruptly changes as the amount of current changes so that the power-line becomes unstable in communication. As a result, we estimate that during the transfer function abruptly changing, communication forbidden time occurs. We are also studying the relationship between this charging phase angle and the communication forbidden time. Figure 5 shows the power-line frequency created under this simulation conditions and that acquired by actual measurement. The simulation conditions are severe as the instantaneous change of the power-line frequency is extreme than the actual measurement. The results of the plot simulation under the above conditions are shown in Fig. 6. Figure 6(a) is a fixed period superimposed chart in which the Superimposed Period is fixed at 10 msec, which is half of the power-line period. Figure 6(b) is the Proposed Chart using the proposed algorithm. Both charts use the same data, but only the Superimposed Period is different. In Fig. 6(a)

Table 2 Simulation condition.

Burst signal interval	2.3 msec
Number of burst signals	80,000 burst signals
Power-line frequency	Average 50 Hz, Standard deviation 0.2 Hz, Change at 218 or 219 msec intervals
Communication forbidden time	Power-line phase angle from 60 to 90 degrees

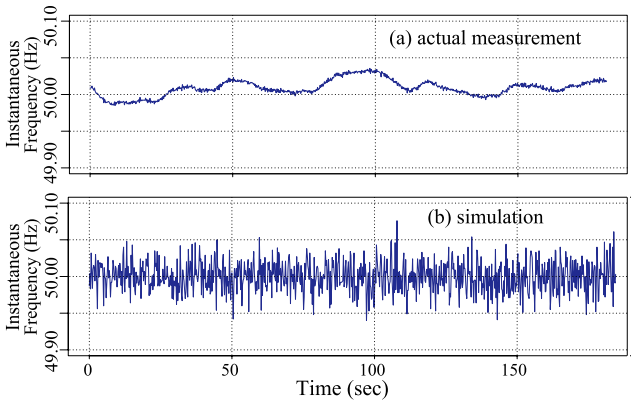

Fig. 5 Power-line frequency simulation.

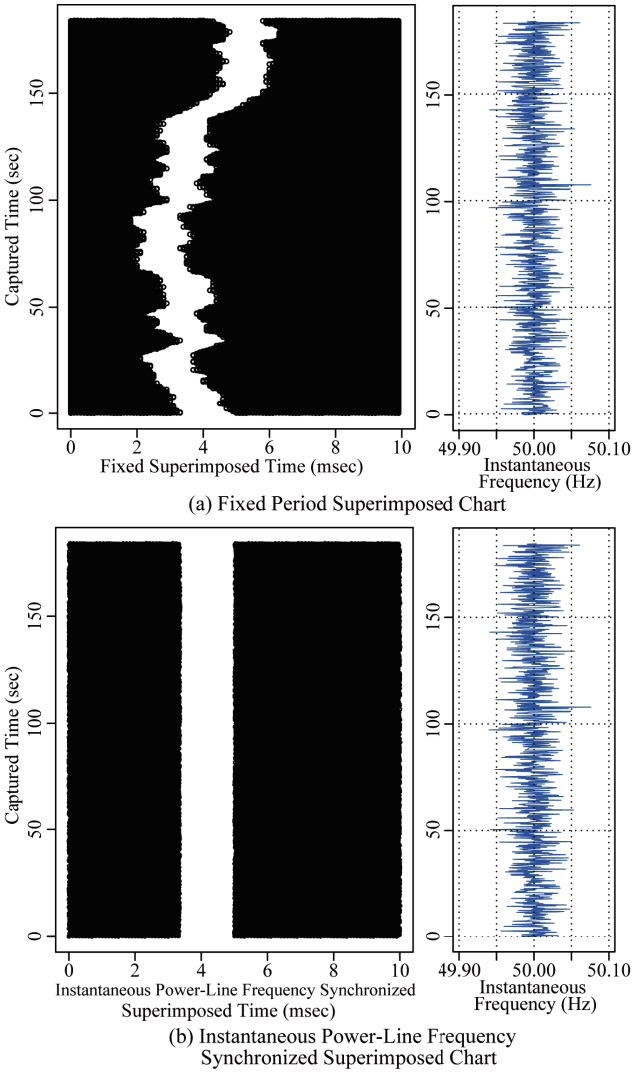

Fig. 6 Plot simulation.

plotted fixedly at 10 msec, the white section indicating the communication forbidden time is winding curved, whereas in Fig. 6(b) of the proposed method synchronized with the instantaneous power-line frequency, it is aligned in the straight line. As shown by this simulation result, we confirmed the effectiveness of the Proposed Chart and its plotting algorithm because the communication forbidden time is aligned vertically than plotting over the fixed period.

4. Verification of Initial Burst Signal Plotting Position Dependence

Although the effectiveness of the algorithm was confirmed by plotting simulation, it is conceivable that the white section of the communication forbidden time appears separately on both sides of the Proposed Chart and it is difficult to analyze accurately because the communication forbidden time is divided. In that case, it is possible to manipulate the position of the communication forbidden time by changing the initial burst signal plotting position. At this time, if the burst signal intervals plotted before the changing are not equal to that after the changing, despite using the same data, analysis results may change. This problem occurs when the initial burst signal plotting position is changed, the instantaneous power-line frequency when the Superimposed Time exceeds the Superimposed Period does not coincide, and is referred to as *Initial Burst Signal Plotting Position Dependence* (for short *IBS-PPD*). In this section we will discuss the IBS-PPD.

4.1 Initial Burst Signal Plotting Position Dependence

Superimposed Time ST_n is sequentially obtained using the previous Superimposed Time ST_{n-1}, and the initial value thereof is the initial burst signal plotting position $IniP$ as shown in Eq. (2). Therefore, if there is no dependence on the initial burst signal plotting position, even if the plotting starts from the different position, each burst signal interval, Superimposed Time difference ΔST, is constant. Further, even if it has the IBS-PPD, if the plotting position difference of each point is negligibly small, it can be analyzed correctly using the Proposed Chat. The next section shows the verification method and the IBS-PPD is verified.

4.2 Verification Method of Initial Burst Signal Plotting Position Dependence

The calculation procedure for verification of the IBS-PPD is shown in Fig. 7, and the verification procedure of the IBS-PPD is shown in Fig. 8. The IBS-PPD verification method will be described in detail with reference to these figures. As preparation, using the same packet capture data and instantaneous power-line frequency, Proposed Charts A and B that differ only in the initial burst signal plotting position $IniP_a$ and $IniP_b$, where let $IniP_a$ be larger than $IniP_b$, are plotted. In this case, the initial burst signal plotting position difference $\Delta IniP$ is obtained by the following:

$$\Delta IniP = IniP_a - IniP_b. \tag{8}$$

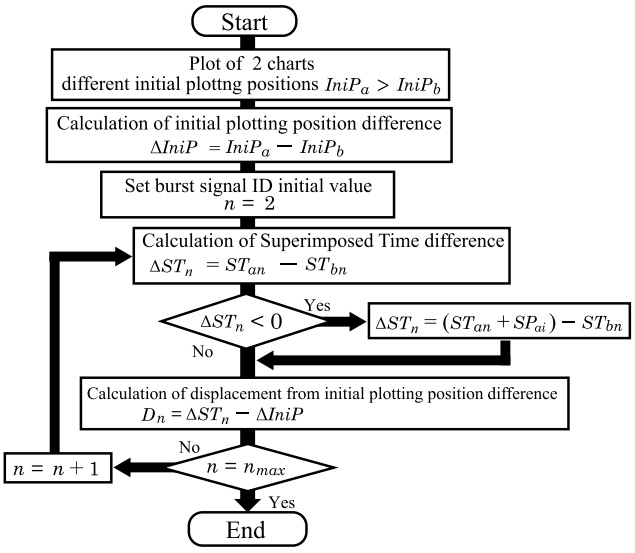

Fig. 7 Calculation procedure of inital burst signal plotting position dependence.

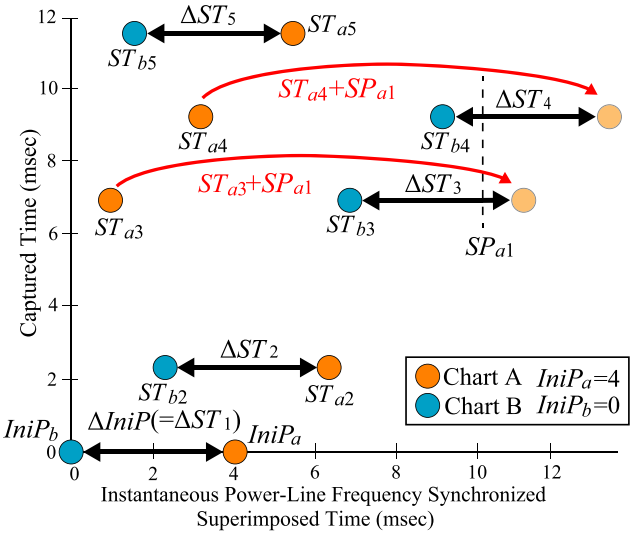

Fig. 8 Verification procedure.

Next, in order to compare the plotted positions of the same n-th burst signal, let the Superimposed Time be ST_{an} and ST_{bn} in the Chart A and B, the Superimposed Time difference ΔST_n of the n-th burst signal is obtained by the following:

$$\Delta ST_n = ST_{an} - ST_{bn}. \tag{9}$$

When n is 3 in Fig. 8, since Superimposed Time ST_{a3} of the Chart A exceeds Superimposed Period SP_{a1}, the exceeded value of ST_{a3} is converted again from 0 on the horizontal axis as shown in **Step 5** of the plotting algorithm. Therefore, ΔST_n becomes a negative value and it is not possible to calculate correctly. In this case, as shown in the red letters in Fig. 8, ΔST_3 is calculated by restoring the value exceeding SP_{a1}. The general formula when ΔST_n becomes negative is as follows:

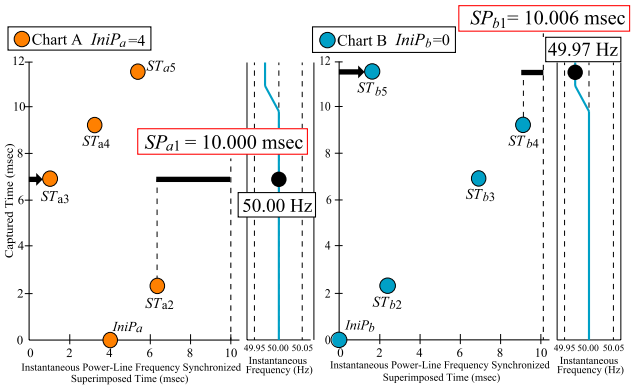

Fig. 9 Chart A and B separately and instantaneous power-line frequency.

$$\Delta ST_n = (ST_{an} + SP_{ai}) - ST_{bn}, \tag{10}$$

where i is the number of times ST_{an} has exceeded SP_{an}. In order to verify the IBS-PPD, let the displacement from the initial burst signal plotting position difference D_n, briefly to be *Displacement,* be the difference between the Superimposed Time difference ΔST_n and the initial burst signal plotting position difference $\Delta IniP$, Displacement D_n is calculated as following:

$$D_n = \Delta ST_n - \Delta IniP. \tag{11}$$

With all burst signals, Displacement D_n is calculated. If the IBS-PPD does not exist, that is, when Displacement D_n is 0 or negligibly sufficiently small, it is no problem even if the initial burst signal plotting position is changed for the evaluation of the communication forbidden time.

Further, the relationship of the IBS-PPD and the Superimposed Period will be discussed. Figure 9 shows the Chart A and B separately shown in Fig. 8 and also shows an example of the instantaneous power-line frequency. As shown in Fig. 9, when the initial burst signal plotting position is changed, the burst signal $\mathrm{ID_n}$ in which the Superimposed Time ST_n exceeds the Superimposed Period SP_n differs between the Chart A and B. In the Chart A, ST_{a3} exceeds SP_{a1}, but ST_{b3} in the Chart B does not exceed SP_{b1} yet. In the Chart B, it exceeds SP_{b1} for the first time at ST_{b5}. In addition, since the instantaneous power-line frequencies when it exceed SP_{a1} and SP_{b1} are 50.00 Hz and 49.97 Hz, respectively, SP_{a1} and SP_{b1} are 10 msec and 10.006 msec, respectively. As this example shows, the instantaneous power-line frequency may be different depending on the timing at which ST_n exceeds SP_n because SP_{an} and SP_{bn} may be different. We will discuss this influence in detail using mathematical formulas. From Eq. (4) of the proposed algorithm **Step 3**, ST_n is calculated using ST_{n-1}, and ST_1 is $IniP$ from Eq. (2). Furthermore, SP_n is subtracted when ST_n exceeds SP_n from Eq. (6) of the proposed algorithm **Step 6**. From the above, ST_{an} in the Chart A can be transformed as follows:

$$\begin{aligned} ST_{an} =& IniP_a + (Int_{Burst\ 2} + Int_{Burst\ 3} + \cdots + Int_{Burst\ n}) \\ & - (SP_{a1} + SP_{a2} + \cdots + SP_{ai}) \\ =& IniP_a + \sum_{k=2}^{n} Int_{Burst\ k} - \sum_{k=1}^{i} SP_{ak}. \end{aligned} \tag{12}$$

Similarly for the Chart B, ST_{bn} can be transformed as follows:

$$ST_{bn} = IniP_b + \sum_{k=2}^{n} Int_{Burst\ k} - \sum_{k=1}^{j} SP_{bk}, \tag{13}$$

where j is the number of times ST_{bn} has exceeded SP_{bn}. Superimposed Time difference ΔST_n in Eq. (9) can be transformed as follows using Eq. (12) and Eq. (13):

$$\begin{aligned} \Delta ST_n &= ST_{an} - ST_{bn} \\ &= IniP_a - IniP_b - \sum_{k=1}^{i} SP_{ak} + \sum_{k=1}^{j} SP_{bk} \\ &= \Delta IniP - \sum_{k=1}^{i} SP_{ak} + \sum_{k=1}^{j} SP_{bk}. \end{aligned} \tag{14}$$

Furthermore, Displacement D_n in Eq. (11) can be obtained by Eq. (14) as follows:

$$\begin{aligned} D_n &= \Delta ST_n - \Delta IniP \\ &= \Delta IniP - \sum_{k=1}^{i} SP_{ak} + \sum_{k=1}^{j} SP_{bk} - \Delta IniP \\ &= \sum_{k=1}^{j} SP_{bk} - \sum_{k=1}^{i} SP_{ak}. \end{aligned} \tag{15}$$

Equation (15) shows that D_n is the cumulative difference of SP_{bn} and SP_{an}, unless SP_{an} and SP_{bn} are the same from the plotting start, the IBS-PPD may occur slightly. When the initial burst signal plotting position is changed, since SP_{an} and SP_{bn} may varies with the change of the instantaneous power-line frequency as shown in Fig. 9, those are almost never the same from the beginning to the end. Furthermore, D_n, which is the cumulative difference between SP_{an} and SP_{bn}, fluctuates to positive and negative because the magnitude relationship of them also changes.

4.3 Verification of Initial Plotting Position Dependence Using Test Bed Data

In this section, the influence of the IBS-PPD is discussed. Specifically, some initial burst signal plotting positions are changed with the same data, and the influence of IBS-PPD is confirmed by evaluating the difference and variation of D_n and the difference between the Proposed Charts. Test bed data is used for confirmation with respect to the IBS-PPD. The test bed system is the same as in Fig. 1. Packets are transmitted for 180 seconds from the TxPC to RxPC at the preset UDP transmission speed of 30 Mbit/s. At the same time, the instantaneous power-line frequency is measured using the digital multimeter. Test bed data was obtained from 5 times measurements. Using the measured 5 data,

Table 3 Maximum Displacement to positive and negative.

(a) Displacement to positive value

$IniP_b$	0				2			4		6
$IniP_a$	2	4	6	8	4	6	8	6	8	8
1st data	0.012935	0.029237	0.026315	0.01826	0.017144	0.014281	0.006806	0.001399	0.0002	–
2nd data	0.003739	0.00734	0.010145	0.012526	0.005841	0.007964	0.010104	0.003883	0.006443	0.002761
3rd data	0.000371	0.004253	0.016895	0.013236	0.009778	0.022301	0.018097	0.017979	0.012969	–
4th data	–	0.002386	0.006908	0.013766	0.004082	0.008604	0.015463	0.004742	0.01138	0.007319
5th data	0.012342	0.017735	0.028073	0.023225	0.012252	0.024435	0.012723	0.013305	0.009574	0.007546

(b) Displacement to negative value

$IniP_b$	0				2			4		6
$IniP_a$	2	4	6	8	4	6	8	6	8	8
1st data	-0.00228	-0.0016	-0.0014	-0.00789	-0.00026	-0.00496	-0.01395	-0.01515	-0.02414	-0.01156
2nd data	-0.0007	–	–	–	–	–	-0.0002	-0.0013	-0.00322	-0.00202
3rd data	-0.02007	-0.02011	-0.00657	-0.0126	-0.00551	-0.002	-0.00427	-0.00056	-0.00202	-0.00834
4th data	-0.00343	-0.00607	-0.00731	-0.00904	-0.0034	-0.00417	-0.00585	-0.00157	-0.00339	-0.00188
5th data	-0.00112	-0.00112	-0.00186	-0.0113	-0.00068	-0.00198	-0.01314	-0.00531	-0.01849	-0.01961

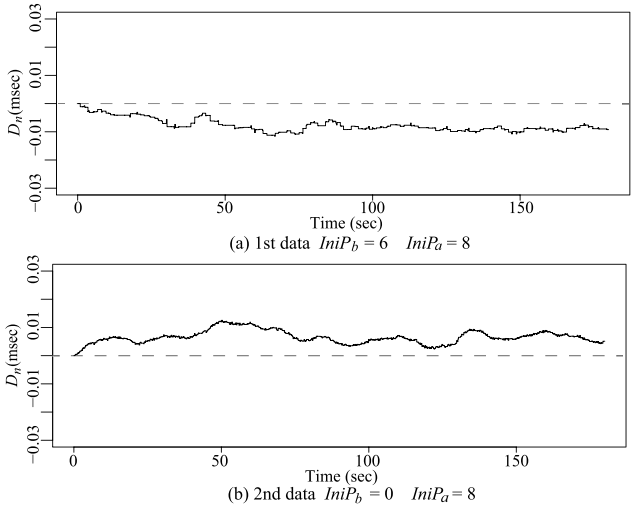

Fig. 10 Example of positive or negative displacement 0.

Displacement D_n was found for all combinations of the initial burst signal plotting position 0, 2, 4, 6 and 8 msec where $IniP_a$ is larger than $IniP_b$ in the Chart A and B. Table 3 shows the maximum Displacement to the positive and to the negative. The symbol of "-" in the tables indicates that there was no positive or negative Displacement value, and the highlighted cells indicate the maximum Displacement of positive and negative, respectively. First, we will discuss no Displacement value. Figure 10 shows the time variations of the Displacement D_n by selecting one by one from the combination where the no positive and negative Displacement. Figure 10(a) shows that when $IniP_a$ is 8 and $IniP_b$ is 6 at the first measurement data, and Fig. 10(b) is the case when $IniP_a$ is 8 and $IniP_b$ is 0 at the second one. Both (a) and (b) do not monotonously increase or monotonically decrease, and the Displacement D_n is repeatedly fluctuating positive and negative value. D_n obtained by Eq. (15) does not monotonically increase or decrease because the instantaneous power-line frequency fluctuates, that is, SP_{an} and SP_{bn} also fluctuate. In addition, when comparing the two figures, Fig. 10(a) with smaller the difference of the initial burst signal plotting position, when $IniP_a$ is 8 and $IniP_b$ is 6, is quantized. When the difference is small, the instantaneous power-line frequencies

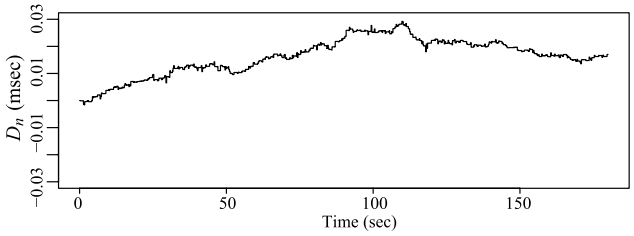

Fig. 11 Time variation when positive displacement is maximum.

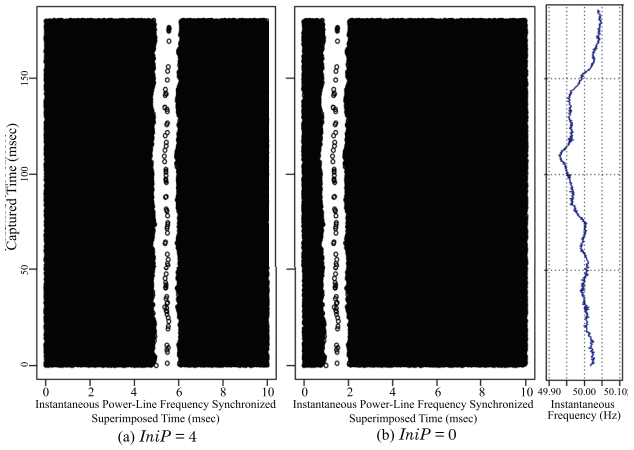

Fig. 12 Proposed Charts when positive displacement is maximum.

sometimes have the same value, that is, the i-th Superimposed Period SP_{an} and the j-th SP_{bn} often have the same value in some cases. For example, assuming that SP_{an} and SP_{bn} have the same value three consecutive times, the difference between SP_{an} of i to $i+2$ and SP_{bn} of j to $j+2$ becomes 0 in Eq. (15), and in order to keep the previous value of the Displacement D_n, the time variation is plotted as quantized. Next, the case of the maximum Displacement will be discussed. The positive maximum Displacement is 0.029237, and the negative one is −0.02414. Assuming that the Superimposed Period is approximately 10 msec, the Displacement with respect to that is within 0.3% at most, in other words, the Displacement is negligibly small. Figure 11 shows the time variation of the Displacement when the positive Displacement is the maximum value. Even in this case, although the Displacement becomes the maximum value at around 110 seconds, the Displacement is fluctuated and does not converge. Figure 12 shows the Proposed Charts when the positive Displacement is the maximum value, and the instantaneous power-line frequency. Fig. 12(a) shows when the initial burst signal plotting position $IniP$ is 4, and (b) shows when $IniP$ is 0. In Fig. 12(a) and (b), each point is plotted on behalf of only the burst signal head packet. Fig. 12(a) and (b) have the maximum Displacement 0.3% in the vicinity of 110 seconds. However, since the Displacement is negligibly small, there is no problem in analyzing the communication situation using the Proposed Chart even if confirming the two figures that changed the initial burst signal plotting position. As an analysis example, we will

discuss in the next section with reference to Fig. 12(a).

5. Analysis Example of Actual Data

We will show an analysis example of the Proposed Chart using packet captured data obtained by the test bed system. By applying the Proposed Chart, it becomes possible to analyze the behavior of the inter-computer communications using PLC which could not be analyzed so far in detail. Figure 13 shows the Proposed Chart in which each point is color-coded based on the number of packets included in the burst signal. Figure 13(a) is the color-coded chart of data measured for 180 second at the preset UDP transmission speed of 30 Mbit/s when the charger is not connected, and Fig. 13(b) is that of Fig. 12(a) based on the number of packets included in the burst signal at RxPC. As described in Sect. 3.1, since each burst signal head packet holds the data of the burst signal included packet number, it is possible to display color-coded points. As shown in Fig. 13, the major color coding is Black when the number of included packets is 1 to 3, Light Blue for 4 to 6, Blue for 7 to 9 and Light Green for 10 to 12. According to the specification of HD-PLC [16], up to 31 packets are included in one burst signal. For this reason, it color-coded so that it can be understood that up to 31 packets are included. First of all, with respect to Fig. 13(a) when the charger is not connected, Light Blue having the included packet number of 4 to 6 is dominant. This is because, as described in Fig. 2(b), the included packet number is 5 or 6 under this measurement condition. Furthermore, there is no communication forbidden time indicated by the white section. Second, with respect to Fig. 13(b), Light Blue is dominant like the case when the charger is not connected. Even when the charger is connected, the number of burst signal included packets is basically the same as when not connected. The characteristic when connected is the occurrence of the communication forbidden time described so far. Focusing on the communication forbidden time in the white section, the duration of the communication forbidden time is approximately 1 msec for this test bet system. Although all 5 or 6 packets that started transmission during the communication forbidden time are not detected, those packets were transmitted together with 5 or 6 packets that are next normally transmitted. After 2.3 msec of the communication forbidden time, there is the Light Green duration of 1 msec which is the same duration as the communication forbidden time. In order to explain in more detail, Fig. 14 which is an enlarged view around 35.65 second on the vertical axis in Fig. 13(b) is also used. The black dotted line in Fig. 14 indicates the communication forbidden time, and the numbers of included packets are indicated at the plotting points before and after that duration. The discussion in this case corresponds to A1 in Fig. 14. The burst signal including 6 packets before the communication forbidden time is transmitted, and after 2.3 msec, it is transmitted within the duration indicated

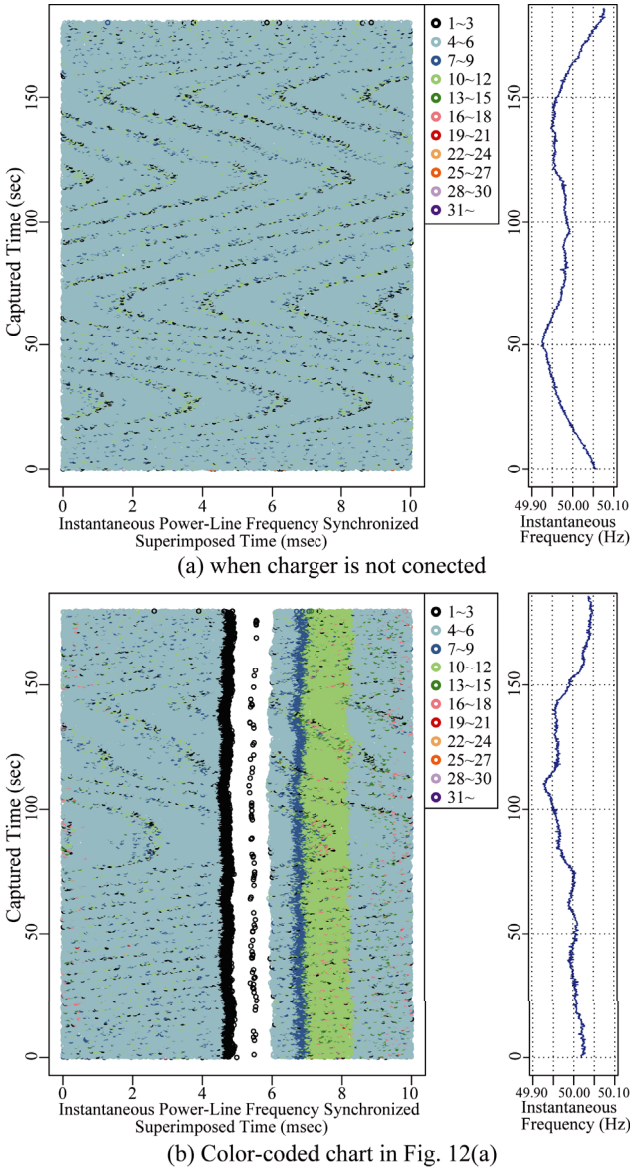

Fig. 13 Color-coded chart based on the number of included packets.

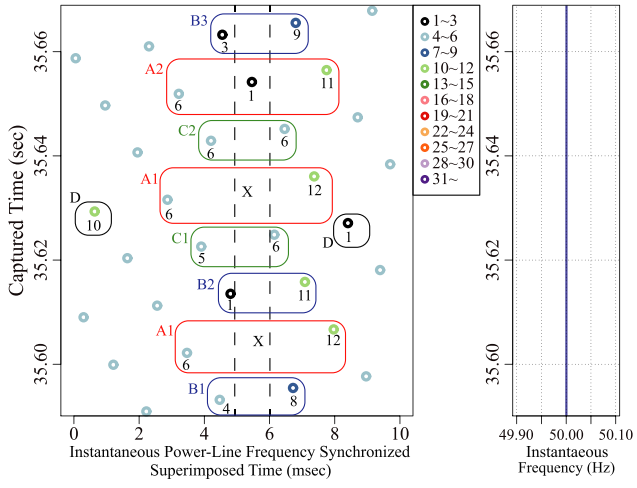

Fig. 14 Enlarged chart of Fig. 13(b).

by "X". Since it is in communication forbidden time, the burst signal is not detected at RxPC. Based on the discussion with MAC layer of the PLC section in Sect. 2.2, the transmitting PLC had transmitted the frame body aggregated 5 or 6 subframes regardless of the communication forbidden time, and recognized that the subframe could not be received normally from the Result Map field in the Acknowledgement sent from the Receiving PLC. And the packets which could not received and the packets which were scheduled to be transmitted were aggregated in the new frame body and transmitted it after communication forbidden time. As described above, it can be estimated by the instantaneous power-line frequency synchronized superimposed chart indicating the state of inter-computers communications. As a point of attention within the communication forbidden time, several packets are detected almost at the center of during the communication forbidden time in Fig. 13(b). The discussion in this case corresponds to A2 in Fig. 14. The interval between the burst signals before and after that point is 2.3 msec like the others. Furthermore, one packet is detected near the center of the communication forbidden time as compared with "X" which is estimated to be transmitted within the communication frobidden time of A1. We estimate that the power-line is instantaneously stabilized near the center of the communication forbidden time, and part of the burst signal transmitted by chance at that time is detected at RxPC. The analysis of this phenomenon is for further study. Next, in Fig. 13(b), immediately before the start of the communication forbidden time, Black with the included packet number 1 to 3 are distributed. When the communication forbidden time starts during the transmission of the burst signal, 1 to 3 packets before starting the communication forbidden time out of the normally included 5 or 6 packets are detected, and the remaining packets being transmitted after the communication forbidden time has started are not detected. Considering that the burst signal interval in this experimental condition is 2.3 msec, there is the Blue duration of 7 to 9 included packets just after 2.3 msec of the Black duration immediately before the communication forbidden time. This can also be implied from that the shapes and durations of the Blue line resemble that of the Black line. The discussion in this case corresponds to B1 to B3 in Fig. 14. In the case of B1, 4 packets out of a total of 6 packets were detected at RxPC before the start of the communication forbidden time, and 8 packets were detected in the next burst signal together with the 2 not-detected packets. In the case of B2 and B3, since the transmission starting time of the burst signal is closer to the start point of the communication forbidden time than B1, the number of packets detected by RxPC before the communication forbidden time is smaller than B1, and is smaller as the communication forbidden time is closer. The not-detected packets are collectively detected after the communication forbidden time. On the other hand, in case of C1 and C2 in Fig. 14, since 5 or 6 packets were normally detected before the communication forbidden time, 6 packets were detected in the next. Considering with MAC layer of the PLC section, since the Transmitting PLC transmits the frame body in which 5 or 6 subframes are aggregated, the subframes in the frame body affected by the communication forbidden time are not detected normally by the Receiving PLC. Furthermore, the Receiving PLC informs the subframe number of unsuccessful reception in the Result Map field of the Acknowledgement, and the Transmitting PLC aggregates and transmits to the next frame body. The above can be estimated from this instantaneous power-line frequency synchronized superimposed chart. Finally, black striped pattern is shown in Fig. 13. A part of the point appears in D in Fig. 14, and 10 packets were detected in the next burst signal. This striped pattern can be inferred from the analysis result of another chart we proposed, called the system specific period superimposed chart [20]. This chart is plotted focusing on that a specific burst signal is vertically aligned at a certain period, called system specific period. Immediately before the burst signals are vertically aligned, there is a short duration where packets are not detected. The duration occurs irrespective of whether or not the charger is connected. As in the case where the communication forbidden time occurs in its study, only about 1 or 2 packets are detected immediately before the duration when packets are not detected. We estimate that a few packets detected by the phenomenon appear as black striped pattern in the Proposed Chart. As described above, it is possible to analyze the influence of the communication forbidden time by the Proposed Chart, and it is effective for evaluating and analyzing the communication quality of inter-computer communications using PLC.

6. Conclusion

The authors showed the communications forbidden time which packets was not detected once a half period of power-line period when AC adapters such as mobile phone chargers are connected to a PLC system. Furthermore, we proposed the instantaneous power-line frequency synchronized superimposed chart in order to visualize the communications forbidden time and evaluate communications quality. In addition, the initial burst signal plotting position dependence was verified, its dependence is negligibly, and even if the initial burst signal plotting position is changed, the relationship between the burst signal intervals on the instantaneous power-line frequency synchronized superimposed chart is guaranteed. The above discussion confirms the effectiveness of the instantaneous power-line frequency synchronized superimposed chart is shown and the example of analysis using that chart is also shown. As future studies, we will analyze the communication situation and quality at the occurrence of the communication forbidden time, the influence of other electronic equipment on PLC and an actual environment communications using the instantaneous power-line frequency synchronized superimposed chart.

References

[1] X. Carcell, Power Line Communications in Practice, Artech House,

Boston, 2006.
[2] HD-PLC Alliance, "HD-PLC," HD-PLC Alliance, http://www.hd-plc.org/, accessed Nov. 8. 2018.
[3] HomePlug Alliance, "HomePlug," HomePlug Alliance, http://www.homeplug.org/, accessed Nov. 8. 2018.
[4] International powerline communications Forum, "UPA," International powerline communications Forum, https://www.ipcf.org/company/upa/universal-powerline-association, accessed Nov. 8. 2018.
[5] IEEE Communications Society Standards Committee, "IEEE Standard for Broadband over Power Line Networks: Medium Access Control and Physical Layer Specifications," IEEE-SA Standards Board, Dec. 2010.
[6] Nikkei Communication, All of High-Speed Power Line Communication, Nikkei BP, Tokyo, 2006 (in Japanese).
[7] A. Papaioannou, and F.-N. Pavlidou, "Evaluation of power line communication equipment in home networks," IEEE Syst. J., vol.3, no.3, pp.288–294, Sept. 2009.
[8] F.J.C. Corripio, J.A.C. Arrabal, L.D. del Rio, and J.T.E. Munoz, "Analysis of the cyclic short-term variation of indoor power line channels," IEEE J. Ssel. Areas Commun., vol.24, no.7, pp.1327–1338, July 2006.
[9] D. Umehara, T. Hayasaki, S. Denno, and M. Morikura, "Influences of periodically switching channels synchronized with power frequency on PLC equipment," J. Communications, vol.4, no.2, pp.108–118, March 2009.
[10] ADCMT, "Digital Multi Meter 7352A/7352E," ADC corporation, http://www.adcmt.com/techinfo/product/intro/i_7352A_E.html, accessed Nov. 13, 2018.
[11] SOURCEFORGE, "iperf 2," Slashdot Media, https://sourceforge.net/projects/iperf2/, accessed Nov. 13, 2018.
[12] SharkFest, "Wireshark," https://www.wireshark.org/, SharkFest, accessed Nov. 13, 2018.
[13] Panasonic, "BL-PA310 Spec.," https://panasonic.jp/p3/p-db/BL-PA310_spec.html, Panasonic, accessed Nov. 13, 2018.
[14] Ubuntu Japanese Team, "Ubuntu Japanese Team," Ubuntu Japanese Team, https://www.ubuntulinux.jp, accessed Nov. 13, 2018.
[15] UNION, "MNR-D," UNION ELECTRIC Co., Ltd. http://uniondk.jp/trans/trans_mnr-d, accessed Nov. 13, 2018.
[16] The Telecommunication technology committee, "Home network Communication Interface for ECHONET Lite (Broadband Wavelet OFDM PLC (HD-PLC))," TTC JJ-300.20, Dec. 2013.
[17] G. Masuda, S. Mori, and H. Shinonaga, "Packet capture analysis of effects of AC adapter in power line communications (V)," IEICE Gen. Conf.'13, p.242, March 2013.
[18] Investigating R & D Committee of regular and emergency load frequency control in the power system, "Regular and emergency load frequency control in the power system," IEEJ Technical Reports, vol.869, pp.66–67, March 2002 (in Japanese).
[19] P.M. Chirlian, "Power supplies," Electronic Circuits: Physical Principles, Analysis, and Design, pp.813–842, McGraw-Hill, New York, 1971.
[20] W. Abe, H. Gotoh, R. Uemura, K. Kita, H. Ishikawa, and H. Shinonaga, "System specific period superimposed chart in PLC system under UDP transmission — Part 2: Verification of system specific period search algorithm under test bed and actual in-phase and out-of-phase communications environments —," IEICE Technical Report, CS2018-72, Nov. 2018.

Kenji Kita received Bachelor of Design degree from Kyushu Institute of Design, Fukuoka, Japan in 2006, and Master of Design, Ph.D. in Design degrees from Kyushu University, Fukuoka, Japan in 2008, 2015, respectively. In 2006, he joined Sharp Corporation, Osaka, Japan, where he was in charge of acoustic design on LCD TV of Southeast Asia model from 2008 to 2010. He was a Lecturer in Malaysia Japan Higher Education Program in University of Kuala Lumpur, Malaysia from April 2013 to March 2016. Since April 2016, he has been an Assistant Professor of Faculty of Science and Engineering, Toyo University, Saitama, Japan.

Hiroshi Gotoh received Bachelor of Science and Engineering from Toyo University, Saitama, Japan in 2018. He is currently in Graduate School of Science and Engineering, Toyo University from April 2018. He has been engaged in the research of PLC systems.

Hiroyasu Ishikawa received a B.E., M.E., and Ph.D. in Communication Engineering from Osaka University, Osaka, Japan in 1989, 1991, and 2001, respectively. He joined the Research and Development Laboratories of Kokusai Denshin Denwa Co., Ltd. (KDD) in 1991, where he has been engaged in the research of digital satellite communication systems, satellite navigation systems, mobile communication systems, wireless LAN systems, digital processing technologies, and software-defined radio technologies. He received the Meritorious Award on Radio from the Association of Radio Industries and Businesses in 2002 for the development of high-speed, long-distance wireless communications systems using the 2.4-GHz ISM band. He was a senior manager of the Wireless Platform Laboratory of KDDI R&D Laboratories from April 2008 to February 2012. He has been a Professor at the College of Engineering, Nihon University, Fukushima, Japan.

Hideyuki Shinonaga received B.E., M.E., and D.E. degrees in Electrical Communications Engineering from Osaka University, Osaka, Japan, in 1979, 1981 and 1995, respectively. In 1981, he joined the Research and Development Laboratories of Kokusai Denshin Denwa (KDD, currently KDDI) Company, Tokyo, Japan, where he was been engaged in research on digital satellite communications, terrestrial radio systems, radio LANfs, ITS and digital cellular systems. He was an Executive Director of KDDI R&D Laboratories from 2002 to 2009. Since April 2009, he has been a Professor of Faculty of Science and Engineering, Toyo University, Saitama, Japan.